

## Inhomogeneous isospin distribution in the reactions of $^{28}\text{Si}+^{112}\text{Sn}$ and $^{124}\text{Sn}$ at 30 and 50 MeV/nucleon

M. Veselsky,<sup>\*</sup> R. W. Ibbotson,<sup>†</sup> R. Laforest,<sup>‡</sup> E. Ramakrishnan,<sup>§</sup> D. J. Rowland, A. Ruangma, E. M. Winchester, E. Martin, and S. J. Yennello

*Cyclotron Institute, Texas A&M University, College Station, Texas 77843*

(Received 9 March 2000; published 21 September 2000)

We have created quasiprojectiles of varying isospin via peripheral reactions of  $^{28}\text{Si}+^{112}\text{Sn}$  and  $^{124}\text{Sn}$  at 30 and 50 MeV/nucleon. The quasiprojectiles have been reconstructed from completely isotopically identified fragments. The difference in  $N/Z$  of the reconstructed quasiprojectiles allows the investigation of the disassembly as a function of the isospin of the fragmenting system. The isobaric yield ratio  $^3\text{H}/^3\text{He}$  depends strongly on  $N/Z$  ratio of quasiprojectiles. The dependences of mean fragment multiplicity and mean  $N/Z$  ratio of the fragments on  $N/Z$  ratio of the quasiprojectile are different for light charged particles and intermediate mass fragments. Observation of a different  $N/Z$  ratio of light charged particles and intermediate mass fragments is consistent with an inhomogeneous distribution of isospin in the fragmenting system.

PACS number(s): 25.70.Mn, 25.70.Pq

There has been significant interest in multifragmentation of excited nuclear matter for many years. While there has been some success in understanding the process of multifragmentation and describing this phenomenon in terms of a liquid gas phase transition [1], those efforts have often treated the nucleus as a single component nuclear liquid. In fact, the nucleus is a two component nuclear liquid. Early work by Lamb [2] laid the foundations for treating the nucleus as a two component system although the results were not connected to multifragmentation. Statistical calculations describing multifragment disassembly predicted that much of the neutron excess would be observed as free neutrons [3]. Thermodynamic calculations by Müller and Serot [4] led us to the idea that, for the very neutron rich systems, there may exist a distribution of the excited nuclear material into a neutron-rich gas and a more symmetric liquid. It is predicted by both lattice gas and mean field calculations [5,6] that fragmentation of a system of asymmetric nuclear material will express the characteristics of a two component system. This would result in a second-order phase transition. Also within a dynamical code, constructed to study influence of charge asymmetry on spinoidal decomposition of nuclear material at subsaturation densities, differences in the fragmentation are seen as a function of isospin asymmetry [7].

The difference of the mean  $N/Z$  ratio of the light charged particles with  $Z_f \leq 2$  (LCPs) and of the intermediate mass fragments with  $Z_f \geq 3$  (IMFs) may be a possible experimental signature of a separation into a gas (resulting mostly in emitted LCPs) and a liquid (IMFs). An enhanced production of neutron-rich H and He isotopes from the neck region has

been seen experimentally in midperipheral collisions [8,9], while a favored emission of more symmetric heavy clusters in the midrapidity region has also been shown [10]. Quite neutron deficient residues have also been seen in intermediate energy reactions [11,12]. Recent results from the reaction of  $^{112,124}\text{Sn}+^{112,124}\text{Sn}$  indicate that the relative abundance of free neutrons increases as the neutron content of the colliding system increases [13]. The present work will demonstrate that, in a well defined system with isotopic identification of all charged fragments, the mean value of the  $N/Z$  ratio of LCPs is more sensitive than mean  $N/Z$  ratio of IMFs to the  $N/Z$  of quasiprojectile. The more asymmetric the system is the stronger it will favor breaking up into still more asymmetric light fragments while the  $N/Z$  ratio of heavier fragments remains relatively insensitive.

This experiment was done with a beam of  $^{28}\text{Si}$  impinging on  $>1$  mg/cm<sup>2</sup> of  $^{112,124}\text{Sn}$  self supporting targets. The beam was delivered at energies 30 and 50 MeV/nucleon by the K500 superconducting cyclotron at the Cyclotron Institute of Texas A&M University. The detector setup is composed of an arrangement of 68 silicon-CsI(Tl) telescopes covering polar angles from 1.64° to 33.6° in the laboratory frame. Each element is composed of a 300  $\mu\text{m}$  surface barrier silicon detector followed by a 3 cm CsI(Tl) crystal. The detectors are arranged in five concentric rings. The geometrical efficiency is more than 90% for each ring. These detectors allow for isotopic identification of light charged particles and intermediate mass fragments up to a charge of  $Z=5$ . A more detailed description of the detectors and electronics can be found in Ref. [14]. Energy calibration of the silicon detectors was achieved with the use of a  $^{228}\text{Th}$  source providing six calibration points from 5.42 to 8.78 MeV. The CsI(Tl) detectors were calibrated from the measured energy loss in the silicon detector of a given particle of a certain mass and charge and from its total kinetic energy calculated with SRIM-96 [15]. In addition, the punch-through points of hydrogen isotopes in CsI(Tl) crystals were also used. The overall procedure gives an energy resolution of typically 3%. More details of the experimental setup and calibration can be found in Ref. [16].

Electronic address: veselsky@comp.tamu.edu; On leave of absence from Institute of Physics of SASc, Bratislava, Slovakia.

<sup>†</sup>Present address: Brookhaven National Laboratory, Brookhaven, NY 11973.

<sup>‡</sup>Present address: Mallinckrodt Institute of Radiology, St. Louis, MO 63110.

<sup>§</sup>Present address: Microcal Software Inc., One Roundhouse Plaza, Northampton, MA 01060.

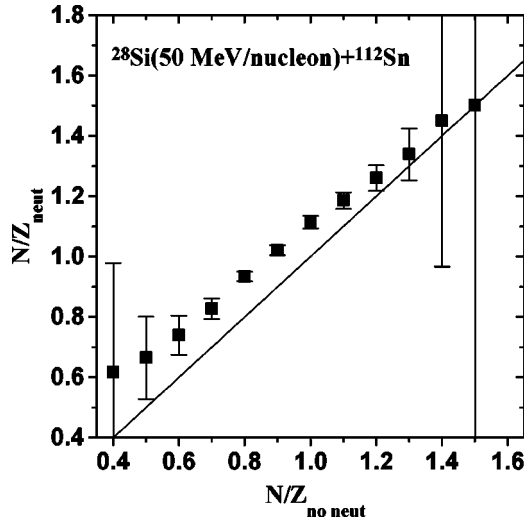


FIG. 1. Average  $N/Z$  ratio of all fragments emitted from the quasiprojectile versus those bound in charged fragments for the reaction  $^{28}\text{Si}(50 \text{ MeV/nucleon}) + ^{112}\text{Sn}$ . Symbols represent the hybrid DIT/SMM calculation. Solid line indicates the case  $N/Z_{\text{neut}} = N/Z_{\text{noneut}}$ .

The total charge of quasiprojectile (QP) was restricted to the values  $Z_{\text{tot}} = 12-15$ . We have required that all detected fragments are isotopically identified. This highly exclusive set of data possesses information on fragmentation of highly excited projectilelike prefragments over a range in isospin that can be measured on an event-by-event basis. Simulations have been done with a hybrid code treating the two stages of the reaction—nucleon exchange and quasiprojectile deexcitation. The first stage of the calculation was simulated with the Monte Carlo code of Tassan-Got [17]. This code implements the model of deep inelastic transfer (DIT) [18]. For the deexcitation of the highly excited quasiprojectile we used the statistical multifragmentation model (SMM) [19]. The quasiprojectile event sequences generated by the DIT code have been used as input of the SMM simulations. The results of the calculation were filtered through the FAUST software replica. This hybrid calculation reproduces very well the quasiprojectile and fragmentation observables in these reactions [20].

In Fig. 1 we show the effect of including emitted neutrons in the calculation of  $N/Z_{\text{QP}}$ . Since the experimental setup cannot detect free neutrons it is important to see if this might bias the data. The  $N/Z_{\text{noneut}}$  is the neutron to proton ratio of the quasiprojectiles simulated using hybrid DIT/SMM simulation and filtered using FAUST software replica. Thus  $N/Z_{\text{noneut}}$  applies to quasiprojectiles where only charged particles are included. The  $N/Z_{\text{neut}}$  is the backtraced total neutron to proton ratio of the primary quasiprojectiles for the same set of events. The line represents equal values for  $N/Z_{\text{neut}}$  and  $N/Z_{\text{noneut}}$ . The data presented on Fig. 1 represent the reaction  $^{28}\text{Si}(50 \text{ MeV/nucleon}) + ^{112}\text{Sn}$ . While there is some deviation from the line due to neutron evaporation, the calculation predicts that  $N/Z_{\text{neut}}$  tracks very well with  $N/Z_{\text{noneut}}$ . The situation is similar also when using  $^{124}\text{Sn}$  target or lower projectile energy. Therefore for the remainder of this paper  $N/Z_{\text{QP}}$  will be  $N/Z_{\text{noneut}}$ .

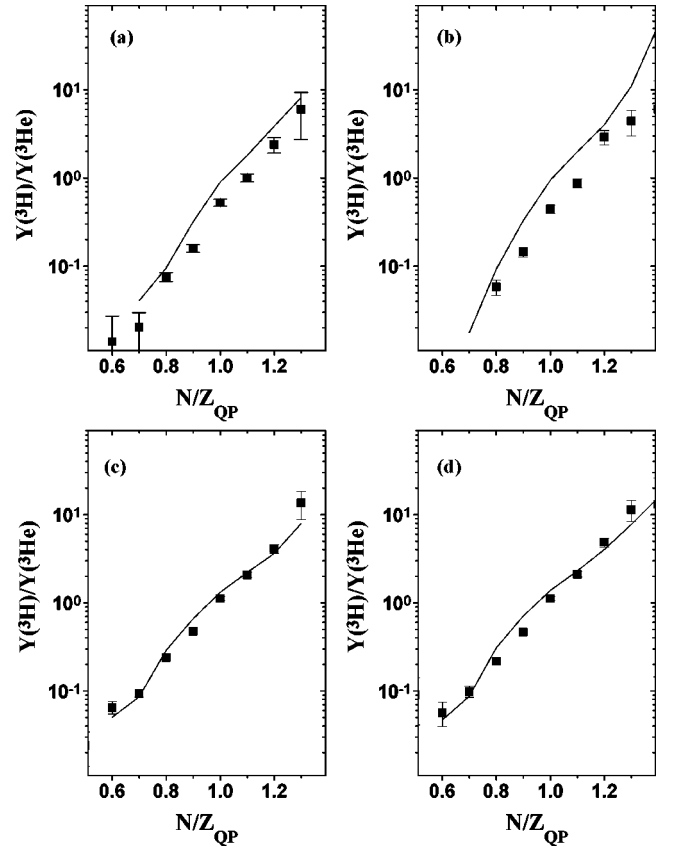


FIG. 2. Isobaric yield ratio  $^3\text{H}/^3\text{He}$  versus  $N/Z_{\text{QP}}$  for the reactions of  $^{28}\text{Si}$  beam with tin targets. (a) 30 MeV/nucleon,  $^{112}\text{Sn}$ , (b) 30 MeV/nucleon,  $^{124}\text{Sn}$ , (c) 50 MeV/nucleon,  $^{112}\text{Sn}$ , (d) 50 MeV/nucleon,  $^{124}\text{Sn}$ . Symbols represent the experimental data. Lines represent the hybrid DIT/SMM calculation.

In Fig. 2 is shown the dependence of the isobaric yield ratio  $^3\text{H}/^3\text{He}$  on  $N/Z_{\text{QP}}$ . The yield ratio  $^3\text{H}/^3\text{He}$  increases as  $N/Z_{\text{QP}}$  increases. Similar effects have been seen in other systems where isotopic or isobaric ratios have been plotted as a function of  $N/Z$  of the reacting system [8,21]. In the present data, the  $N/Z_{\text{QP}}$  is the reconstructed  $N/Z$  of all detected charged particles. If one fits the data with an exponential function  $\exp(a_1 + a_2 N/Z_{\text{QP}})$ , the slope  $a_2$  is nearly identical for the reaction with the  $^{112}\text{Sn}$  target as with the  $^{124}\text{Sn}$  target. The slopes presented in Table I show that this increase in the yield ratio  $^3\text{H}/^3\text{He}$  as a function of  $N/Z_{\text{QP}}$  is much larger than would be expected from the change in  $N/Z_{\text{QP}}$  alone. While the integrated values on the two targets are different when broken down by the  $N/Z_{\text{QP}}$  the behavior is

TABLE I. Values of the slope parameter  $a_2$  obtained from the fit  $\log_{10}(Y(^3\text{H})/Y(^3\text{He})) = a_1 + a_2(N/Z)_{\text{QP}}$ .

Reaction	Projectile energy		
	[MeV/nucleon]	$a_2(\text{exp})$	$a_2(\text{calc})$
$^{28}\text{Si} + ^{112}\text{Sn}$	30	$3.99 \pm 0.38$	$3.89 \pm 0.16$
$^{28}\text{Si} + ^{124}\text{Sn}$	30	$4.13 \pm 0.11$	$4.57 \pm 0.24$
$^{28}\text{Si} + ^{112}\text{Sn}$	50	$3.16 \pm 0.18$	$3.15 \pm 0.16$
$^{28}\text{Si} + ^{124}\text{Sn}$	50	$2.83 \pm 0.27$	$3.10 \pm 0.11$

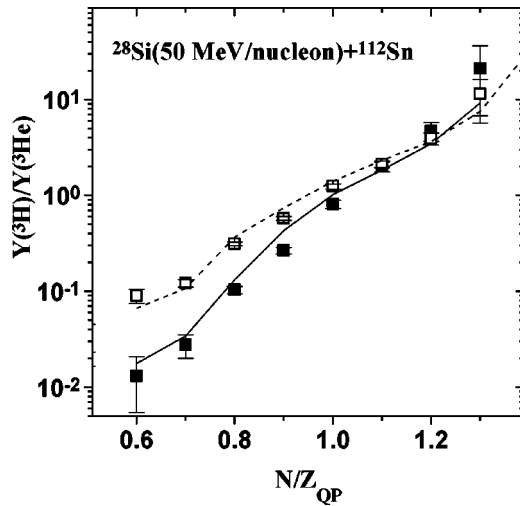


FIG. 3. Isobaric yield ratio  ${}^3\text{H}/{}^3\text{He}$  versus  $N/Z_{\text{QP}}$  for the reaction  ${}^{28}\text{Si}(50\text{MeV/nucleon})+{}^{112}\text{Sn}$ . Symbols represent the experimental data for two different cuts on apparent excitation energy per nucleon (solid squares,  $\epsilon^* < \epsilon_{\text{mean}}^*$ ; open squares,  $\epsilon^* > \epsilon_{\text{mean}}^*$ ). Lines represent the hybrid DIT/SMM calculation (solid line,  $\epsilon^* < \epsilon_{\text{mean}}^*$ ; dashed line,  $\epsilon^* > \epsilon_{\text{mean}}^*$ ).

similar. If one looks at the difference with bombarding energy, the dependence of yield ratio  ${}^3\text{H}/{}^3\text{He}$  on  $N/Z_{\text{QP}}$  is lessened at the higher energy. This is consistent with the lattice-gas calculation [5] that predicted that the  ${}^3\text{H}/{}^3\text{He}$  ratio would be enhanced at lower temperatures for the system with excess neutrons. At relatively high temperatures above 12 MeV, the ratio would asymptotically approach the  $N/Z_{\text{QP}}$  value. The hybrid DIT/SMM calculations reproduce the experimental yield ratio  ${}^3\text{H}/{}^3\text{He}$  rather well. This shows that the statistical multifragmentation model correctly describes the influence of isospin on the production rates of fragments. The overall  ${}^3\text{H}/{}^3\text{He}$  ratio for the reaction with the  ${}^{112}\text{Sn}$  target is 0.25 and with the  ${}^{124}\text{Sn}$  target is 0.35 to 30 MeV/nucleon and 0.44 and 0.62, respectively, at 50 MeV/nucleon. This increase in the yield of neutron-rich fragments with an increase in the  $N/Z$  of the reacting system is consistent with other studies of isobaric ratios [13,21]. What Fig. 2 demonstrates is that this is an integrated feature and merely shows that the system created with the neutron-rich target is more neutron rich. But when one takes the  ${}^3\text{H}/{}^3\text{He}$  ratio as a function of the  $N/Z_{\text{QP}}$ , the behavior may be seen much more clearly.

In Fig. 3 we have investigated the effect of excitation energy on the  ${}^3\text{H}/{}^3\text{He}$  ratio. The solid squares represent all events, where the excitation energy is less than the mean excitation energy per nucleon of the events included in Fig. 2(c) ( ${}^{28}\text{Si}+{}^{112}\text{Sn}$  at 50 MeV/nucleon,  $\epsilon^* \leq 5.5$  MeV/nucleon). The open squares represent the events whose excitation energy is greater than the mean excitation energy. The slope is steeper for events at lower excitation energies. We observed a similar behavior for all reactions regardless of the bombarding system or beam energy. The results of hybrid calculation (lines) are again in reasonable agreement with experiment. Further work investigating the excitation energy dependence of  ${}^3\text{H}/{}^3\text{He}$  ratio is forthcoming [22].

In Fig. 4(a) we show the multiplicity of charged particles

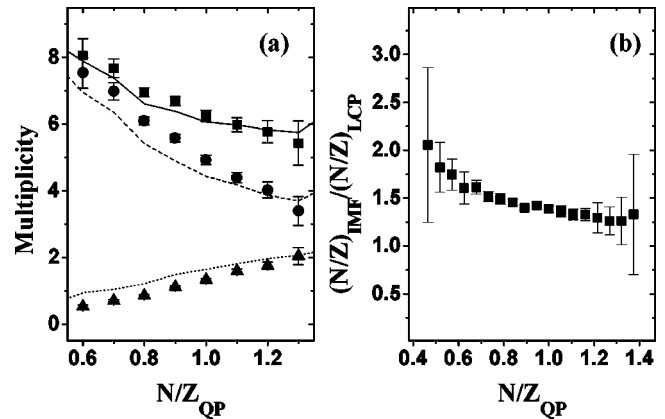


FIG. 4. (a) Multiplicity of charged fragments (squares), LCPs (circles), and IMFs (triangles) versus  $N/Z_{\text{QP}}$ . Corresponding lines represent the hybrid calculation. (b) Experimental ratio of the mean values of  $N/Z$  of LCPs and IMFs versus the  $N/Z_{\text{QP}}$ . Data are given for the reaction  ${}^{28}\text{Si}(50\text{MeV/nucleon})+{}^{112}\text{Sn}$ .

versus  $N/Z_{\text{QP}}$ , again for the reaction  ${}^{28}\text{Si}+{}^{112}\text{Sn}$  at 50 MeV/nucleon. The squares represent the multiplicity of all charged particles. The multiplicity of charged particles increases as  $N/Z_{\text{QP}}$  decreases. This is then broken down into the multiplicity of light charged particles (circles) and the multiplicity of intermediate mass fragments (triangles). Here we can see that the multiplicity of LCPs increases with decreasing  $N/Z_{\text{QP}}$ . Meanwhile the multiplicity of IMFs increases as  $N/Z_{\text{QP}}$  increases. The situation is similar for all cases. The results are identical for different targets at the same projectile energy. The dependence of the multiplicity of IMFs on  $N/Z_{\text{QP}}$  is practically the same for all cases. The increase in overall multiplicity of charged particles with increasing beam energy is similar to the increase of the multiplicity of LCPs. The results of the hybrid calculation (lines) are consistent with the experiment. Again the presented information is consistent with, but much more illustrative than, previous works where the difference in isospin of the excited system was only approximately known on average [23,24]. Previous works show that the multiplicity of IMFs as a function of multiplicity of charged particles increases for the more neutron rich system. While this is true, the present data show that this is concurrent with the decrease in the multiplicity of LCPs for neutron-rich systems. Our data show that this effect weakens at higher energies, possibly towards the disappearance, which was seen by Miller *et al.* [24] at much a higher energy. Our data would be consistent also with the temperature dependence predicted by lattice-gas model calculations [5].

In Fig. 4(b) we show the ratio  $N/Z_{\text{IMF}}/N/Z_{\text{LCP}}$  as a function of  $N/Z_{\text{QP}}$ . The ratio  $N/Z_{\text{IMF}}/N/Z_{\text{LCP}}$  decreases with increasing  $N/Z_{\text{QP}}$ . As there are fewer neutrons available the excess protons go into the smaller fragments rather than the larger fragments. The least neutron-rich quasiprojectiles with  $N/Z_{\text{QP}} \approx 0.5$  prefer to breakup into very neutron deficient LCPs and much more symmetric IMFs. This inhomogeneous isospin distribution washes out rapidly as  $N/Z_{\text{QP}}$  approaches the region of  $\beta$  stability. Such a behavior may be understood when taking into account that the  $N/Z$  range of detected LCPs is much wider than the  $N/Z$  range of IMFs where usually only a few stable and nearly stable isotopes are pro-

duced. The observed inhomogeneous isospin distribution is likely caused by more favorable energy balance of the deposition of proton excess into LCPs, either free protons or light proton-rich clusters (see Figs. 2,3). When extrapolating this trend towards very neutron-rich quasiprojectiles the isospin distribution would most likely reappear again in the form of neutron-rich LCPs and more symmetric IMFs. Such an extrapolation is consistent with the predicted asymmetric liquid gas phase transition [4] where in addition to the inhomogeneous isospin distribution a spatial separation of fractions with different isospin occurs. For neutron rich nuclei, such a phase transition is predicted at the values of  $N/Z$  exceeding 1.5, corresponding to proton concentrations of 40% or less. The data presented here raises the question of whether an analogous separation of the system into subsystems with different isospin may be expected for very neutron-deficient fragmenting systems. Our data support such a scenario. Nevertheless, one has to take into account that the studied fragmenting system is quite small and the number of possible exit channels may play an important role in the determination of final partition of fragments. The influence of the secondary decay was estimated by simulations where only an emission of hot fragments took place. The number of simulated events, where all fragments have been isotopically resolved, decreased for a given overall number of simulated events by 50% at projectile energy 30 MeV/nucleon and by 90% at 50 MeV/nucleon. This may be explained by a lower mean multiplicity and higher mean mass and charge of hot fragments, which in our case leads to a lower number of simulated events where only fragments up to boron ( $Z_f \leq 5$ ) are emitted. Nevertheless, the absence of secondary emission stage did not influence the ratio  $N/Z_{\text{IMF}}/N/Z_{\text{LCP}}$  as a function of the  $N/Z_{\text{QP}}$ , which remained unchanged within

statistical errors. This implies that the isospin dependence of the ratio  $N/Z_{\text{IMF}}/N/Z_{\text{LCP}}$  is, according to the statistical multifragmentation model, determined in the hot multifragmentation stage. The neutron emission does not seem to influence the presented data dramatically, as may be seen in Fig. 1.

We have demonstrated that systems of varying isospin can be created and studied by projectile fragmentation reactions. The spread in  $N/Z$  of the fragmenting system is larger than the difference between the reacting systems. This can be observed by the complete isotopic reconstruction of the quasiprojectile. We have investigated the isobaric yield ratio  ${}^3\text{H}/{}^3\text{He}$  as a function of  $N/Z$  ratio of the fragmenting system. The yield ratio  ${}^3\text{H}/{}^3\text{He}$  increases as  $N/Z_{\text{QP}}$  increases. This depends more significantly on the fragmenting system than on the reacting system. At higher energies this dependence is lessened. We conclusively demonstrated that the multiplicity of charged particles depends on the isospin of the fragmenting system. As the  $N/Z_{\text{QP}}$  decreases the overall multiplicity of charged particles increases. The multiplicity of LCPs increases dramatically while the multiplicity of IMFs decreases. This effect is less significant at higher bombarding energy. We have also presented evidence of an inhomogeneous isospin distribution of the fragmenting system into two fractions with different values of  $N/Z$ .

The authors wish to thank the Cyclotron Institute staff for the excellent beam quality. This work was supported in part by the NSF through Grant No. PHY-9457376, the Robert A. Welch Foundation through Grant No. A-1266, and the U.S. Department of Energy through Grant No. DE-FG03-93ER40773. M.V. was partially supported through Grant No. VEGA-2/5121/98.

- 
- [1] J. E. Finn, *et al.*, Phys. Rev. Lett. **49**, 1321 (1982).  
 [2] D. Q. Lamb, J. M. Lattimer, C. J. Pethick, and D. G. Ravenhall, Nucl. Phys. **A360**, 459 (1981).  
 [3] J. Randrup and S. E. Koonin, Nucl. Phys. **A356**, 223 (1981).  
 [4] H. Müller and B. D. Serot, Phys. Rev. C **52**, 2072 (1995).  
 [5] Ph. Chomaz and F. Gulminelli, Phys. Lett. B **447**, 221 (1999).  
 [6] B. A. Li and C. M. Ko, Nucl. Phys. **A618**, 498 (1997).  
 [7] V. Baran, M. Colonna, M. Di Toro, and A. B. Larionov, Nucl. Phys. **A632**, 287 (1998).  
 [8] J. F. Dempsey *et al.*, Phys. Rev. C **54**, 1710 (1996).  
 [9] L. G. Sobotka, Phys. Rev. C **50**, R1272 (1994); L. G. Sobotka, J. F. Dempsey, and R. J. Charity, *ibid.* **55**, 2109 (1997).  
 [10] E. Ramakrishnan, H. Johnston, F. Gimeno-Nogues, D. J. Rowland, R. Laforest, Y-W. Lui, S. Ferro, S. Vasal, and S. J. Yennello, Phys. Rev. C **57**, 1803 (1998).  
 [11] K. A. Hanold, D. Bazin, M. F. Mohar, L. G. Moretto, D. J. Morrissey, N. A. Orr, B. M. Sherrill, J. A. Winger, G. J. Wozniak, and S. J. Yennello, Phys. Rev. C **52**, 1462 (1995).  
 [12] M. Gonin *et al.*, Phys. Rev. C **42**, 2125 (1990).  
 [13] H. S. Xu *et al.*, Phys. Rev. Lett. **85**, 716 (2000).  
 [14] F. Gimeno-Nogues *et al.*, Nucl. Instrum. Methods Phys. Res. A **399**, 94 (1997).  
 [15] J. P. Biersack and J. F. Ziegler, SRIM-96, Stopping and Range of Ion in Matter.  
 [16] R. Laforest, E. Ramakrishnan, D. J. Rowland, A. Ruangma, E. M. Winchester, E. Martin, and S. J. Yennello, Phys. Rev. C **59**, 2567 (1999).  
 [17] L. Tassan-Got and C. Stéfan, Nucl. Phys. **A524**, 121 (1991).  
 [18] J. Randrup, Nucl. Phys. **A307**, 319 (1978); **A327**, 490 (1979); **A383**, 468 (1982).  
 [19] J. P. Bondorf, A. S. Botvina, A. S. Iljinov, I. N. Mishustin, and K. Sneppen, Phys. Rep. **257**, 133 (1995).  
 [20] M. Veselsky, R. W. Ibbotson, R. Laforest, E. Ramakrishnan, D. J. Rowland, A. Ruangma, E. M. Winchester, E. Martin, and S. J. Yennello, submitted to Phys. Rev. C, nucl-ex/0002007.  
 [21] S. J. Yennello *et al.*, Phys. Lett. B **321**, 14 (1994); H. Johnston, T. White, J. Winger, D. Rowland, B. Hurst, F. Gimeno-Nogues, D. O'Kelly, and S. J. Yennello, *ibid.* **371**, 186 (1996).  
 [22] M. Veselsky, R. W. Ibbotson, R. Laforest, E. Ramakrishnan, D. J. Rowland, A. Ruangma, E. M. Winchester, E. Martin, and S. J. Yennello, submitted to Phys. Lett. B, nucl-ex/0003004.  
 [23] G. J. Kunde *et al.*, Phys. Rev. Lett. **77**, 2897 (1996).  
 [24] M. L. Miller, O. Bjarki, D. J. Magestro, R. Pak, N. T. B. Stone, M. B. Tonjes, A. M. Vander Molen, G. D. Westfall, and W. A. Friedman, Phys. Rev. Lett. **82**, 1399 (1999).